University of Groningen

Characterization method of formability properties of zinc alloy coating on a metal substrate

Pei, Yutao T.; Ahmadi, Masoud

(12) INTERNATIONAL APPLICATION PUBLISHED UNDER THE PATENT COOPERATION TREATY (PCT)

(54) Title: CHARACTERIZATION METHOD OF FORMABILITY PROPERTIES OF ZINC ALLOY COATING ON A METAL SUBSTRATE

(57) Abstract: The present invention relates to a method for the characterisation of formability properties of a zinc alloy coating on a metal substrate and a metal substrate comprising a zinc alloy coating. The method for the characterisation of formability properties of a zinc alloy coating on a metal substrate, the zinc alloy coating containing one or more alloying elements selected from the group consisting of Mg, Al, Ni each with a content of at least 0.3 weight % and at most 10 weight %, optionally one or more additional elements selected from the group consisting of Si, Sb, Pb, Ti, Ca, Mn, Sn, La, Ce, Cr, or Bi, wherein the content by weight of each additional element in the metallic coating is less than 0.3 weight %, inevitable impurities, the remainder being zinc, the zinc alloy coating having a microstructure comprising a primary zinc phase and binary eutectic and/or ternary eutectic phases, wherein Electron Backscatter Diffraction (EBSD) is used to determine a crystallographic orientation-dependent strain hardening exponent (n) of the zinc alloy coating microstructure.

WO 2021/038102 A1

Characterization method of formability properties of zinc alloy coating on a metal substrate

The invention relates to a method for the characterisation of formability properties of a zinc alloy coating on a metal substrate and a metal substrate comprising a zinc alloy coating.

Zinc-coated steels produced via hot-dip galvanization (HDG) process are regarded as the vital materials for household, construction and automotive industries. By addition of elements such as aluminum and magnesium to the conventional pure zinc coatings, the resultant ZnAlMg coatings offer superior corrosion resistance and friction/wear performance. Nevertheless, these recent hot-dip ZnAlMg coatings currently deliver rather low cracking resistance once subjected to forming processes. Microstructural damages of ZnAlMg coatings lead to cracking in severely deformed areas and result in the formation of large cracks and subsequently deteriorate the in-service corrosion resistance. Some studies have been undertaken to increase the cracking resistance of such coatings.

In EP3369838, for example, a zinc alloy plated steel sheet with good bending workability was disclosed, having a microstructure of a ZnAlMg coating with greater than 50% of the primary zinc phases having a preferred zinc orientation [0001].

In JP2010255084, the crack resistance was improved by adding 0.005 to 0.2% by weight of nickel to a metal coating further comprising 1 to 10% by weight of aluminum and 0.2 to 1% by magnesium weight to alter the microstructure of the alloy.

Although these patents provide some indication how to prevent cracking based on the microstructure, the formation mechanisms of these microstructural damages and hence, preventing measures, are not well understood.

This is hampered by the fact that a method to determine the formation mechanisms related to the microstructures is not yet well defined. Hence, there is a need for a method to assess the cracking tendency of zinc based coatings, especially ZnAlMg coatings, and to derive a metal substrate with a zinc alloy with a low tendency towards microcracking.

Therefore it is an objective of the invention to provide a method for the characterization of formability properties of a zinc alloy coating on a metal substrate.

It is another objective of the invention to provide a metal substrate with a zinc alloy coating with favorable formability properties.

2

In a first aspect according to the invention there is provided a method for the characterisation of formability properties of a zinc alloy coating on a metal substrate

- the zinc alloy coating containing one or more alloying elements selected from the group consisting of Mg, Al, Ni each with a content of at least 0.3 weight % and at most 10 weight %, optionally one or more additional elements selected from the group consisting of Si, Sb, Pb, Ti, Ca, Mn, Sn, La, Ce, Cr, or Bi, wherein the content by weight of each additional element in the metallic coating is less than 0.3 weight %, inevitable impurities, the remainder being zinc,
- the zinc alloy coating having a microstructure comprising a primary phase and a binary eutectic and/or ternary eutectic phase,
- wherein Electron Backscatter Diffraction (EBSD) is used to determine a crystallographic orientation-dependent strain hardening exponent (n) of the zinc alloy coating microstructure.

The inventors surprisingly found that the method according to the invention providing a crystallographic orientation-dependent strain hardening exponent (n) as obtained from EBSD had a high correlation to the formation of crack initiation in the zinc alloy coating and therefore can be used as a measure for cracking. The crystallographic orientation-dependent strain hardening exponent (n) may be determined for all phases of the microstructures, of, *e.g.* primary zinc phase, binary eutectic phase and ternary eutectic phase. Preferably, the crystallographic orientation-dependent strain hardening exponent (n) is at least determined for the primary zinc phase. The tendency for cracking of the zinc alloy is related to the micro ductility of the coating. As micro ductility behaviours could be described with the strain hardening exponent (n) for all microstructures in the zinc alloy, the method according to the invention is a solution to reveal and analyse which microstructural phases are most detrimental for crack initiation. The crystallographic orientation-dependent strain hardening exponent (n) can be obtained directly from EBSD or via a combination of EBSD and nanoindentation tests.

EBSD is well known in the field and related experimental settings are described in ISO13067:2011. The zinc alloy has a hexagonal close-packed crystal structure (HPC). This HPC packing of the zinc alloy allows to determine the strain hardening exponent (n) with respect to the crystal orientation from EBSD measurements, which surprisingly provided a good indication for cracking.

It was observed for example, that the binary eutectic phase exhibited on average lower strain hardening exponents then the primary zinc phase or ternary eutectic phase,

3

which corresponds to the general observation that the binary eutectic phase is more prone to cracking. Moreover, the cracking tendency between primary zinc phase with different strain hardening exponents can also be derived from the method according to the invention. Hence, the crystallographic orientation-dependent strain hardening exponent (n) provides a way to describe the cracking tendency for all phases in the zinc alloy coating of the metal substrate, and shows that a microstructure with a low n value has a higher likelihood to show cracking.

It should be noted that in principle the method according to the invention may be used for a zinc alloy coating on any metal substrate, *e.g.* a metal or metal alloy, but in most cases will be a steel strip or a steel blank. For instance Interstitial Free (IF) steels and Bake Hardening (BH) steels for the manufacturing of automotive outer panels, or tinplate for Drawn and Wall Ironing (D&I) applications, for food and beverage packaging.

In a preferred embodiment a Schmid factor (m) of the zinc alloy coating microstructure is determined. The Schmid factor (m) may be determined for all phases of the microstructures, *e.g.* primary zinc phases, binary eutectic phase and ternary eutectic phase. Preferably, the Schmid factor (m) is at least determined for all primary zinc phase. It was found by the inventors that the Schmid factor gave an additional indication for the cracking tendency of the coating, especially when considering the primary zinc phase under strain conditions. It was found that the primary zinc phase with a high Schmid factor can bear the imposed deformation without cracking. Hence the Schmid factor provides an additional indication for the cracking tendency of zinc alloys on a metal substrate under strain. Without wishing to be bound by theory, the inventors believe that the Schmid factor is indicative of the principle slip system, a primary zinc phase with low Schmid factor serves as cracking site, whereas a primary zinc phase with high Schmid factor undergoes a deformation mechanism which stops the propagation of the cracks. This rescue mechanism was specifically observed for cracks propagating into the primary zinc phases.

The Schmid factor was determined from the EBSD analysis. The Schmid factor (m) map of the areas was calculated. For obtaining the Schmid factor (m) associated with each zinc phase, the principle zinc slip systems including all the equivalent crystallographic families were considered and the corresponding Schmid maps were calculated and plotted according to tensile principle stress tensor along loading direction. By this process, the Schmid factor (m) of each cracked and non-cracked zinc phase was determined.

In a preferred embodiment, an orientation angle (θ) between the c-axis of hcp crystal of the primary zinc phase and the loading direction is determined.

4

The orientation angle (θ) was found to be a factor important for the deformation mechanisms of the zinc alloy. This orientation angle (θ) can be obtained from the inverse pole figure (IPF) orientation maps generated on the EBSD data as well known to a person skilled in the art. Accordingly, for each primary zinc phase, orientation angle (θ) between the c-axis of HCP zinc crystal and the loading direction was determined. It was found that the orientation of the basal plane of the primary zinc phase was preferably oriented parallel to the tensile load direction, to reduce cracking.

In a preferred embodiment of the invention, the strain hardening exponent (n) is determined with nanoindentation tests (ISO 14577-4:2016). The crystallographic orientation-dependant strain hardening exponent (n) associated with each indent was calculated using EBSD and raw nanoindentation data by the method described by Dao et al, Computational modeling of the forward and reverse problems in instrumented sharp indentation, Acta Mater. 49 (2001) 3899–3918. doi:10.1016/S1359-6454(01)00295-6. As such the local mechanical properties of each individual phase within the coating could be determined.

In a preferred embodiment the strain hardening exponent (n) of the primary zinc phases is obtained from the orientation angle (θ) via the following equation $n = a\theta^4 - b\theta^3 + c\theta^2 - d\theta + e$, wherein

- $1.0 \times 10^{-8} < a < 1.8 \times 10^{-8}$
- $1.5 \times 10^{-6} < b < 3 \times 10^{-6}$
- $5 \times 10^{-4} < c < 1.5 \times 10^{-3}$
- $1 \times 10^{-4} < d < 8 \times 10^{-4}$
- $0.27 < e < 0.32$

preferably

- $1.2 \times 10^{-8} < a < 1.6 \times 10^{-8}$
- $2.0 \times 10^{-6} < b < 2.5 \times 10^{-6}$
- $8 \times 10^{-4} < c < 1.2 \times 10^{-3}$
- $3 \times 10^{-4} < d < 6 \times 10^{-4}$
- $0.28 < e < 0.30$

more preferably

$n = 1.428 \times 10^{-8}\theta^4 - 2.233 \times 10^{-6}\theta^3 + 1.027 \times 10^{-4}\theta^2 - 4.631 \times 10^{-4}\theta + 0.29$,

wherein θ is ranging from $0 - 90°$, as determined with EBSD as described above.

By using this fourth order equation, the strain hardening exponent (n) of the primary zinc phases can be determined from θ, which significantly simplifies the method according to the invention as θ, and hence n can be easily acquired from EBSD

5

measurements alone. The variables a,b,c,d and e are characteristic for the zinc alloy coating and can be empirically determined from an indented sample. For each indented primary zinc phase, the orientation angle (θ) between the c-axis of HCP zinc crystal and the loading direction (surface normal for nanoindentation) as determined by EBSD was plotted versus the corresponding local strain-hardening index (n) as determined by nanoindentation. The procedure was repeated for all the indented zinc phases. From these measurements, the exact numbers for the variables a, b, c, d and e can be obtained to establish a relationship between θ and n for the specific zinc alloy composition. After establishing the variables for the zinc alloy coating, n can be easily obtained from the samples by EBSD only.

In a second aspect according to the invention there is provided a metal substrate comprising a zinc alloy coating, the zinc alloy coating containing one or more alloying elements selected from Mg, Al, Ni each with a content of at least 0.3 weight % and at most 10 weight %, optionally one or more additional elements selected from among Si, Sb, Pb, Ti, Ca, Mn, Sn, La, Ce, Cr, or Bi, wherein the content by weight of each additional element in the metallic coating is less than 0.3 weight %, inevitable impurities, the remainder being zinc, wherein the microstructure of the zinc alloy coating comprises primary zinc phases and a binary and/or ternary eutectic phase, wherein the primary zinc phases have a crystallographic orientation-dependant strain hardening exponent (n) of at least 0.29 as determined by the method as described above.

It was found that a metal substrate with a zinc alloy coating with a primary zinc phase with a higher n not only has a low tendency towards cracking, but may also rescue cracks initiated in other primary zinc phases or eutectic phases. The primary zinc phases has a n of at least 0.29, preferably an n of at least 0.33, more preferably an n of at least 0.34, most preferably an n of at least 0.35. Although not particularly limited, a suitable upper limit for the n of the primary zinc phases is 1.00, as a primary zinc phase with a n above 1.00 would be unlikely to obtain according to standard production method.

In a preferred embodiment, the primary zinc phases of the zinc alloy coating has a Schmid factor m between 0.01 – 0.5, preferably between 0.33 – 0.5, more preferably between 0.34 – 0.5, most preferably between 0.35 – 0.5. The cracking tendency of a primary zinc phase decreases with an increase in the Schmid factor.

In a preferred embodiment at least 55% of the primary zinc phases of the zinc alloy coating have a θ > 45 °, preferably θ > 60 °, more preferably θ > 65 °, it was observed that primary zinc phases having a θ above 45° showed less cracking and were able to rescue initiated cracks in other phases. Hence, preferably at least 55% of the primary zinc phases have a θ > 45 °, preferably θ > 60 °, more preferably θ > 65 ° to

6

ensure that the overall integrity of the zinc alloy coating is maintained, more preferably at least 65% of the primary zinc phases have a $\theta > 45$ °, preferably $\theta > 60$ °, more preferably $\theta > 65$ °, most preferably at least 75% of the primary zinc phases have a $\theta > 45$ °, preferably $\theta > 60$ °, more preferably $\theta > 65$ °.

5   In a preferred embodiment at least 55% of the primary zinc phases of the zinc alloy coating have a crystallographic orientation-dependant strain hardening exponent n >0.33, preferably n>0.34, more preferably n>0.35. It was observed that primary zinc phases having n above 0.33 showed less cracking and were able to rescue initiated cracks in other phases. Without wishing to be bound by theory, it is believed that the
10   different crystallographic orientation of primary zinc phases possess different magnitudes of local strain hardening exponent as a result of HCP mechanical anisotropy. Accordingly, if more than 75% of primary zinc phases in the zinc alloy have an unfavourable orientations with respect to loading direction, exhibiting n <0.33, this will result in significant cracking during tensile/bending deformation;
15   Hence, preferably at least 75% of the primary zinc phases have a n >0.33, preferably n>0.34, more preferably n>0.35 to ensure that the overall integrity of the zinc alloy coating is maintained, more preferably at least 80% of the primary zinc phases have a n >0.33, preferably n>0.34, more preferably n>0.35.

       In a preferred embodiment at least 55 % of the primary zinc phases have a Schmid
20   factor m > 0.32, preferably m>0.33, more preferably m>0.35. It was observed that primary zinc phases having a m above 0.32 showed less cracking and were able to rescue initiated cracks in other phases. Hence, preferably at least 55% of the primary zinc phases have a m > 0.32, preferably m>0.33, more preferably m>0.35 to ensure that the overall integrity of the zinc alloy coating is maintained, more preferably at least 65%
25   of the primary zinc phases have a m > 0.32, preferably m>0.33, more preferably m>0.35, most preferably at least 75% of the primary zinc phases have a m > 0.32, preferably m>0.33, more preferably m>0.35. The primary zinc phases with a low Schmid factor (m<0.32) lack a dislocation motion for plastic deformation, and therefore are more likely to experience cracking.

30   In a preferred embodiment the zinc alloy coating comprises 5 to 35 % of a binary eutectic phase. It was also found by the inventors that most cracks initiated from the binary eutectic phase. The binary eutectic phase also showed a low n, on average below 0.10, showing a high tendency for cracking and a low tendency for rescuing cracks of neighbouring phases. Hence, the presence of binary eutectic phase is preferably
35   maintained between 5 - 35%, more preferably between 5 – 20%, more preferably between 5 – 10%.

7

In this range, initiated cracks in the binary eutectic phase can still be rescued sufficiently by the surrounding phases to maintain the overall integrity of the zinc alloy coating on the metal substrate.

In an alternative embodiment, the zinc alloy coating is free from binary eutectic phase. As most cracks initiate in the binary eutectic phase having a n well below 0.3, on average below 0.10, a zinc alloy coating free from binary eutectic phase is believed to have significantly less cracking.

In a preferred embodiment the zinc alloy coating comprises 0.3 – 5 weight % Al and 0.3 – 5 weight % Mg, more preferably the zinc alloy coating comprises 1 – 2 weight % Al and 1-2 weight% Mg, as such a coating has improved corrosion resistance, stone chipping resistance as compared to conventional zinc coatings.

In a preferred embodiment the zinc alloy coating is a hot dip coating. Although the zinc alloy coating can be applied on the metal substrate in all common methods as known to a person skilled in the art, the metal substrate according to the invention preferably has preferably a zinc alloy coating made by hot-dip coating. Hot-dip coating is well known to a person skilled in the art and has the advantage that it is a reliable and relatively cheap method to apply a zinc alloy coating to at least one side of the metal substrate.

In a preferred embodiment the zinc alloy coating microstructure comprises phases with varying strain hardening exponents, wherein at least 70% of the phases with a crystallographic orientation-dependant strain hardening exponent n < 0.33 are surrounded by phases with a crystallographic orientation-dependant strain hardening exponent n > 0.33. It was found by the inventors that initiation of cracks in the alloy coating could either end up as a crack or could be rescued, leading to an overall acceptable coating layer. As elaborated already, the propagation of cracks involve phase boundaries. Hence, a crack could initiate in a phase with a low n, *e.g.* binary eutectic phase, and could propagate in a phase with a high n, *e.g.* a primary zinc phase. In case the phases with a n below 0.33 are surrounded by phases with a n of at least 0.33, it was found that the propagation of the crack is halted, thereby rescuing the crack formation and maintaining an overall good zinc alloy coating.

The invention is now further described based on the figures and non-limiting examples.

FIG. 1. Shows a schematic representation of microstructural cracking behaviour within ZnAlMg coatings.

FIG. 2 Shows Zn HCP crystal orientation with the loading parallel to the rolling direction (RD). 2a shows Zn HCP crystal orientation favoured for cracking resistance,

with a high m value (0.5), 2b depicts Zn HCP crystal orientation favoured for cracking resistance, with a medium m value (0.32 – 0.45) and FIG 2 (c) shows Zn HCP crystal orientation leading to cracking.

FIG. 3. Depicts the EBSD results of a cracked area after 10% strain subjected to uniaxial tension, including image quality (IQ), IQ plus inverse pole figure (IPF), corresponding Schmid map and HCP crystals of the critical numbered phases.

FIG. 4. Shows the principal zinc slip systems.

FIG. 5. Shows the n-value distribution for three samples (I1, I2, C1) and their EBSD Image Quality Map

FIG. 1. Shows stage I of a cracking path that begun with a nucleation of tiny micro-cracks in $MgZn_2$ platelets of binary eutectic phase as the result of strain localization. The binary eutectic phase has a low n of about 0.08 and is therefore prone to cracking. As the deformation proceeds, these micro-cracks coalesce and grow mostly perpendicular to binary eutectic platelets (e.g. stage (II) in FIG. 1). When the crack reaches the interfaces between the primary Zn phases and the binary eutectic phase, there might be two situations according to the in-situ evaluations performed earlier. The first circumstance is that the adjacent Zn phase exhibits an orientation close to [0001] perpendicular to the loading direction delivering $\theta > 60°$ and/or $m > 0.32$, in accordance to the claims. In this situation, the primary slip systems of Zn phase are activated by easy dislocation motion and subsequently ductile plastic deformation takes place instead of cleavage cracking (assuming the force direction is parallel to RD). Consequently, the crack is arrested in the primary zinc phase boundary. If the adjacent Zn phase possesses an orientation with HCP c-axis parallel to the loading direction (see Fig. 2c) and incorporates low m and n, serving as a favourable site for the propagating crack (e.g. cracked Zn phase No. 2 at stage III, Fig. 1). In particular, by increasing of θ (the orientation angle of HCP c-axis with respect to the loading direction) from 0 to 90°, cleavage becomes less dominant, and principle ductile deformation mechanisms including basal dislocation slip effectively activate and prevent crack propagation. It should be stated that, FIG. 1 delivers the typical cracking mechanisms of ZnAlMg coatings; however, an individual crack may also form in a zinc phase with unfavorable orientation (m < 0.32) without prior nucleation in the binary eutectic phase. Hence, by the method according to the invention, the cracking behaviour of a zinc alloy coating can be easily measured and predicted by analysing n. The other parameters, m and θ provide additional information to the cracking mechanism leading to a complete picture.

FIG 3. Depicts the EBSD results of a cracked area after 10% strain subjected to uniaxial tension, including image quality (IQ), IQ plus inverse pole figure (IPF),

9

corresponding Schmid map and HCP crystals of the critical numbered phases. From the EBSD results it can be observed that Zn phases with low m and low n experienced transgranular cracking during tensile test. For instance, phase no. 1 having c-axis almost parallel to loading direction or RD (θ=2.1°), exhibited a very low strain hardening exponent (n=0.289) and also low Schmid factor (m=0.03), oriented unfavourably and consequently experienced cracking. On the other hand, phase no. 3 possessing strain hardening exponent (n=0.368), and high Schmid factor (m=0.44), exposed as a favourable orientation to accommodate plastic deformation without enduring cracking. In addition, the formed cracks in phases no. 1 and 2, are arrested at the boundaries of adjacent phases with high m-factor.

These EBSD results were obtained according to the method according to the invention. A metal substrate (HSLA grade steel) with a zinc alloy coating (Zn1.6Al1.6Mg) was prepared for nanoindentation and electron backscatter diffraction (EBSD). For this purpose, a square sample (1×1 cm) was cut from the coated metal sheets. The surface of the zinc alloy coated samples was slightly mechanically polished using 1 µm diamond suspension and water-free lubricant on a Struers MD Nap disc for 3-5 minutes to obtain relatively smooth surface. Thereafter, the sample was flat ion milled for 15 minutes by means of an ion polisher (JEOL IB-19520CCP) in order to attain a good surface quality. The in-situ SEM tensile and bending specimens were also prepared with the same procedure given above, before performing the tests.

Nanoindentation tests were conducted utilizing MTS Nano Indenter XP® with Berkovich tip using the continuous stiffness measurement (CSM) mode. Load controlled indentations with an applied force of 3 mN and spacing of 8 µm between the indents were performed on the coating microstructure.

In order to obtain the equation to correlate theta with n, more than 200 indentations in randomly selected three regions were applied in order to sufficiently capture all the existing phases of the microstructure (primary zinc, binary eutectic and ternary eutectic phases) with a good statistical representation. For each indent on the coating microstructure a label was assigned. Strain hardening exponents (n) associated with each labeled indent were then calculated using raw nanoindentation data as described above.

EBSD measurements on the indented regions of the coating were conducted. For this, the sample was placed in a SEM chamber with 70° tilting angle. The region of interest was selected and a working distance of 12-15 µm was applied. A step size of 200 nm and accelerating voltage of 25 kV were used to acquire EBSD patterns.

EBSD measurement was conducted on the cracked areas of specimens subjected to in-situ tensile and bending tests. The obtained EBSD results were analyzed by means of EDAX-TSL OIM™ Analysis 8 software. The image quality (IQ), inverse pole figure (IPF) orientation maps were generated on the EBSD data on the indented regions. Accordingly, for each primary zinc phase, orientation angle (θ) between the c-axis of HCP zinc crystal and the loading direction (surface normal for nanoindentation) was determined and plotted versus the corresponding local strain-hardening exponent (n) of each labeled zinc phase which was achieved previously by nanoindentation. The procedure was repeated for all the indented zinc phases. Ultimately, a fourth order polynomial expression was fitted on the obtained cure to establish a relationship between θ and n. For the alloy coating of the sample containing Zn, 1.6% Al and 1.6% Mg, it was found that $a=1.428\times10^{-8}$, $b=2.233\times10^{-6}$, $c=1.027\times10^{-4}$, $d=4.631\times10^{-4}$ and $e=0.29$, giving the relation n to theta as $n=1.428\times10^{-8}\theta^4 -2.233\times10^{-6}\theta^3+ 1.027\times10^{-4}\theta^2-4.631\times10^{-4}\theta+0.29$

Separate EBSD analysis was performed on the cracked areas of microstructure undergone bending and tensile test. In addition to image quality (IQ) and inverse pole figure (IPF) maps, the Schmid factor (m) map of the areas was calculated. For obtaining the Schmid factor (m) associated with each zinc phase, the principle zinc slip systems including all the equivalent crystallographic families were considered and the corresponding Schmid maps were calculated and plotted according to tensile principle stress tensor along rolling direction (RD). By this process, the Schmid factor (m) of each cracked and non-cracked zinc phase was achieved.

Having the HCP zinc crystal orientation of each cracked and non-cracked phases after bending/tensile tests by EBSD analysis, θ values were calculated for associated phases. The θ values were determined with respect to tensile loading, parallel to RD. Afterwards, each measured θ value was used to calculate corresponding n-values using the expression as defined above.

FIG 4 shows the principle Zn slip systems including all the equivalent crystallographic families which were considered to calculate the corresponding Schmid maps, which was plotted according to tensile principle stress gradient along rolling direction (RD), as described also in R. Parisot, et al., Deformation and Damage Mechanisms of Zinc Coatings on Hot-Dip Galvanized Steel Sheets: Part I. Deformation Modes, Metall. Mater. Trans. A Phys. Metall. Mater. Sci. 35 A (2004) 797–811 and C. Tomé et.al, The yield surface of hcp crystals, Acta Metall. 33 (1985) 603–621.

11

The obtained results for primary zinc phases on a metal substrate with a zinc alloy coating after being subjected to tensile and bending according to method of the invention is shown in the table below.

5   Table 1 Detailed crystallographic orientation and micro-mechanical information of all labeled phases.

Test	Area no.	Zn phase no.	Average phase orientation	Orientation angle, θ (°)	Schmid factor, m	Strain hardening exponent, n	Cracked
Tensile	1	1	$(6\,\bar{12}\,6\,\bar{1})[1\,0\,\bar{1}\,0]$	2.1	0.03	0.289	Yes
	1	2	$(3\,6\,\bar{9}\,\bar{1})[11\,\bar{9}\,\bar{2}\,3]$	14.5	0.25	0.298	Yes
	1	3	$(\bar{37}\,1\,36\,2)[3\,\bar{5}\,2\,22]$	85.3	0.44	0.368	No
	1	4	$(\bar{5}\,4\,1\,15)[8\,\bar{41}\,49\,5]$	63	0.42	0.335	No
Bending	1	1	$(\bar{35}\,32\,3\,3)[\bar{9}\,\bar{12}\,21\,2]$	8.5	0.14	0.292	Yes
	1	2	$(0\,1\,\bar{1}\,\bar{23})[11\,6\,\bar{17}\,1]$	86.4	0.49	0.371	No
	2	1	$(\bar{6}\,\bar{9}\,15\,5)[\bar{11}\,9\,2\,\bar{3}]$	19.1	0.29	0.304	Yes
	2	2	$(10\,12\,\bar{22}\,\bar{1})[6\,\bar{5}\,\bar{1}\,22]$	77	0.47	0.346	No
	3	1	$(\bar{4}\,11\,\bar{7}\,3)[\bar{6}\,1\,5\,0]$	8.4	0.14	0.292	Yes
	3	2	$(\bar{4}\,1\,3\,0)[\bar{4}\,14\,\bar{10}\,3]$	15.3	0.26	0.299	Yes
	3	3	$(2\,11\,\bar{13}\,\bar{2})[10\,\bar{6}\,\bar{4}\,3]$	22.1	0.3	0.309	Yes
	3	4	$(\bar{5}\,4\,1\,0)[\bar{3}\,\bar{6}\,9\,\bar{2}]$	12.6	0.21	0.296	Yes

It can be derived from the table that primary zinc phases with a theta above 45, a Schmid factor above 0.32 and/or a strain hardening exponent above 0.33 do not crack.

10   Next, three zinc coated steel samples (I1, I2 and C1) were prepared with hot dip galvanising at a temperature of 460 - 470 °C. The wiping speed for sample C1 was 20 times higher than for sample I1 and I2. The samples were analysed with EBSD to obtain n, m and θ values and were subjected to a tensile test until a true strain of 0.1. θ-values, varying from 0 – 90 ° with respect to tensile direction were obtained by post-processing 15   of EBSD results. The n-values of the grains and the distribution (as shown in FIG. 5.) were obtained via the equation $n = 1.428 \times 10^{-8}\theta^4 - 2.233 \times 10^{-6}\theta^3 + 1.027 \times 10^{-4}\theta^2 - 4.631 \times 10^{-4}\theta + 0.29$

12

Cracking quantification and fraction of phases were measured by image analysis

It can been seen that the inventive samples I1 and I2, having at least 75% of primary phase crystals with an n > 0.33 leads to significantly less cracking, and shorter average crack length, than the sample C1 having less than 75% of the primary phase crystals with n > 0.33.

Sample	coating	n > 0.33	n > 0.34	θ > 45	θ > 60	m > 0.32	BE	total cracks	crack length
I1	Zn-2.5Al-1.5Mg	89%	67%	87%	75%	95%	<1 %	5	3,6 μm
I2	Zn-1.6Al-1.6Mg	84%	49%	82%	67%	92%	21%	26	6,4 μm
C1	Zn-1.6Al-1.6Mg	70%	23%	66%	39%	88%	22%	92	21,4 μm

CLAIMS

1. A method for the characterisation of formability properties of a zinc alloy coating on a metal substrate,

   - the zinc alloy coating containing one or more alloying elements selected from the group consisting of Mg, Al, Ni each with a content of at least 0.3 weight % and at most 10 weight %, optionally one or more additional elements selected from the group consisting of Si, Sb, Pb, Ti, Ca, Mn, Sn, La, Ce, Cr, or Bi, wherein the content by weight of each additional element in the metallic coating is less than 0.3 weight %, inevitable impurities, the remainder being zinc,

   - the zinc alloy coating having a microstructure comprising a primary zinc phase and binary eutectic and/or ternary eutectic phases,

   - wherein Electron Backscatter Diffraction (EBSD) is used to determine a crystallographic orientation-dependent strain hardening exponent (n) of the zinc alloy coating microstructure, wherein an orientation angle (θ) between the c-axis of hcp crystal of the primary zinc phase and the loading direction is determined, and wherein n is determined from the orientation angle (θ) via an equation $n = a\theta^4 - b\theta^3 + c\theta^2 - d\theta + e$, wherein

     - $1.0 \times 10^{-8} < a < 1.8 \times 10^{-8}$
     - $1.5 \times 10^{-6} < b < 3 \times 10^{-6}$
     - $5 \times 10^{-4} < c < 1.5 \times 10^{-3}$
     - $1 \times 10^{-4} < d < 8 \times 10^{-4}$
     - $0.27 < e < 0.32$,

2. The method according to claim 1, wherein a Schmid factor (m) of the zinc alloy coating microstructure is determined.

3. The method according to claim 1 or 2, wherein the strain hardening exponent (n) is determined with nanoindentation tests.

4. The method according to any of the claims 1 – 3, wherein a, b, c, d and e of the equation $n = a\theta^4 - b\theta^3 + c\theta^2 - d\theta + e$ are determined by plotting the orientation angle (θ) as determined by EBSD versus the corresponding local strain-hardening index (n) as determined by nanoindentation.

14

5. The method according to any of the claims 1 - 4, wherein the strain hardening exponent (n) of the primary zinc phases is obtained from the orientation angle (θ) via the following equation n $=a\theta^4 - b\theta^3 + c\theta^2 - d\theta + e$, wherein

- $1.2 \times 10^{-8} < a < 1.6 \times 10^{-8}$
- $2.0 \times 10^{-6} < b < 2.5 \times 10^{-6}$
- $8 \times 10^{-4} < c < 1.2 \times 10^{-3}$
- $3 \times 10^{-4} < d < 6 \times 10^{-4}$
- $0.28 < e < 0.30$

more preferably n $=1.428 \times 10^{-8}\theta^4 - 2.233 \times 10^{-6}\theta^3 + 1.027 \times 10^{-4}\theta^2 - 4.631 \times 10^{-4}\theta + 0.29$.

6. A metal substrate comprising a zinc alloy coating, the zinc alloy coating containing one or more alloying elements selected from the group consisting of Mg, Al, Ni each with a content of at least 0.3 weight % and at most 10 weight %, optionally one or more additional elements selected from the group consisting of Si, Sb, Pb, Ti, Ca, Mn, Sn, La, Ce, Cr, or Bi, wherein the content by weight of each additional element in the metallic coating is less than 0.3 weight %, inevitable impurities, the remainder being zinc, wherein the microstructure of the zinc alloy coating comprises primary zinc phases and a binary and/or ternary eutectic phase, wherein the primary zinc phases have a crystallographic orientation-dependant strain hardening exponent (n) of at least 0.29, as determined by any of the claims 1 – 5, and wherein at least 75% of the primary zinc phases have a crystallographic orientation-dependant strain hardening exponent n > 0.33.

7. The metal substrate comprising a zinc alloy coating according to claim 6, wherein the primary zinc phases have a Schmid factor m between 0.01 – 0.5.

8. The metal substrate comprising a zinc alloy coating according to claim 6 or 7, wherein at least 55% of the primary zinc phases have a θ > 45 °, preferably θ > 60 °, more preferably θ > 65 °.

9. The metal substrate comprising a zinc alloy coating according to any of claims 6 – 8, wherein at least 55 % of the primary zinc phases have a Schmid factor m > 0.32, preferably m>0.33, more preferably m>0.35.

10. The metal substrate comprising a zinc alloy coating according to any of the claims 6 - 9, wherein the zinc alloy coating comprising 5 to 35 % of a binary eutectic phase.

5

11. The metal substrate comprising a zinc alloy coating according to any of the claims 6 – 9, wherein the zinc alloy coating is free from binary eutectic phase.

12. The metal substrate comprising a zinc alloy coating according to any of the claims 6 - 11, wherein the zinc alloy coating comprises 0.3 – 5 weight % Al and

10   0.3 – 5 weight % Mg.

13. The metal substrate comprising a zinc alloy coating according to any of the claims 6 - 12, wherein the zinc alloy coating is a hot dip coating.
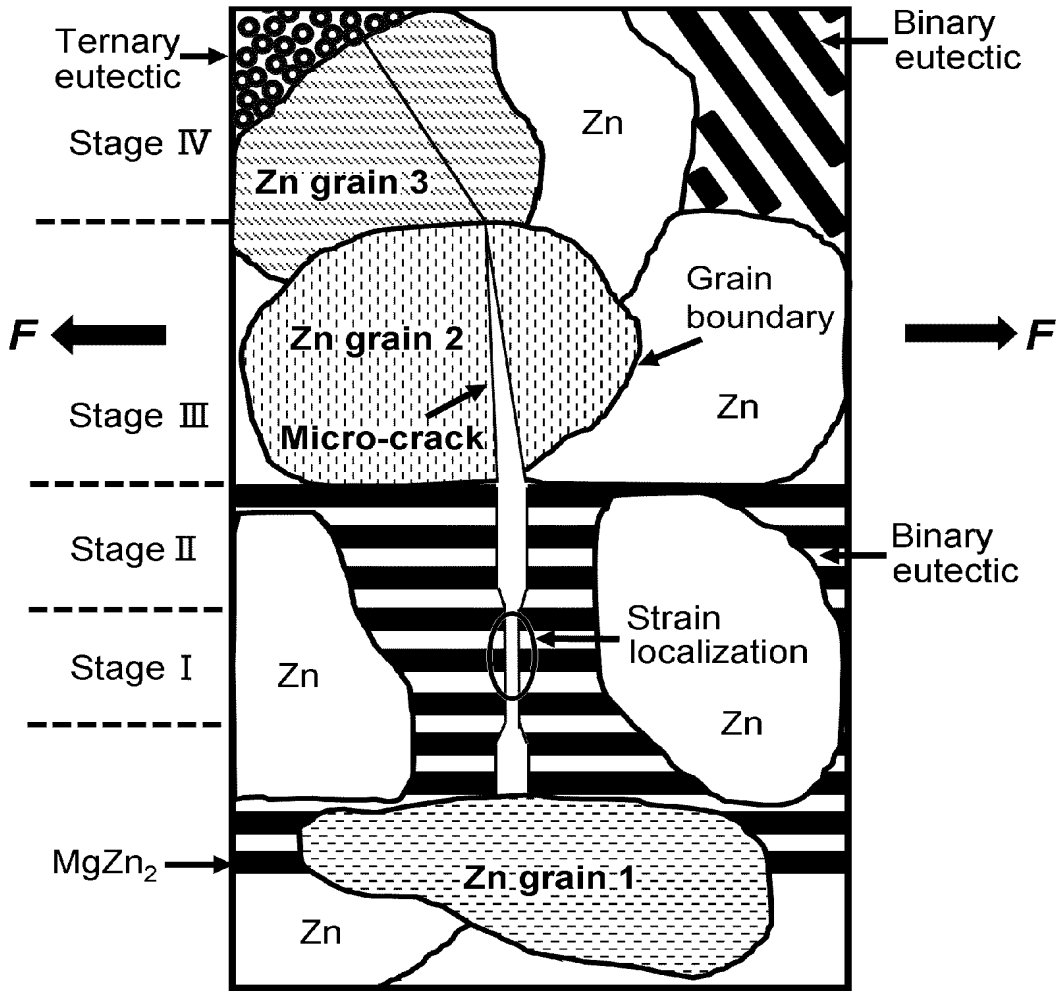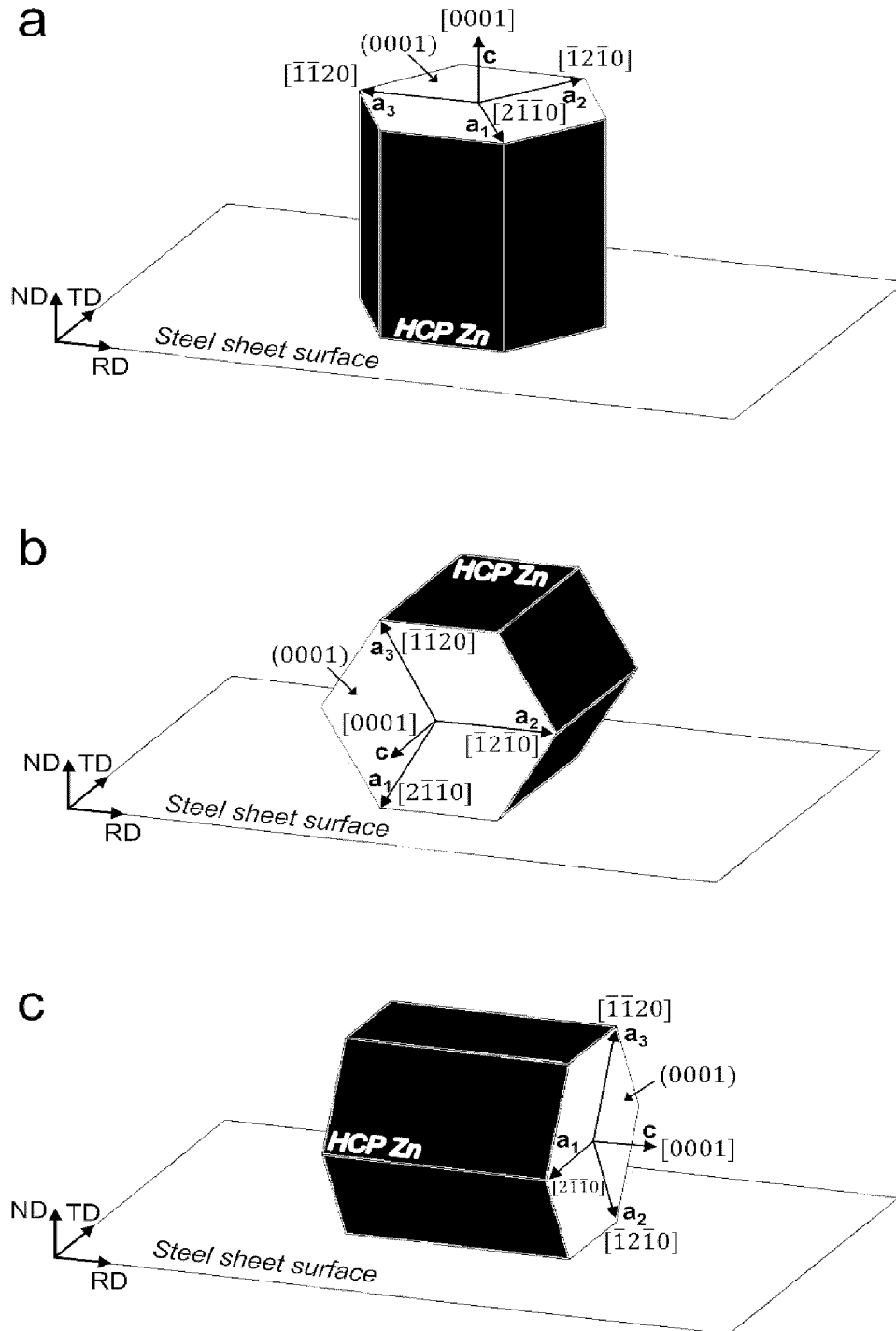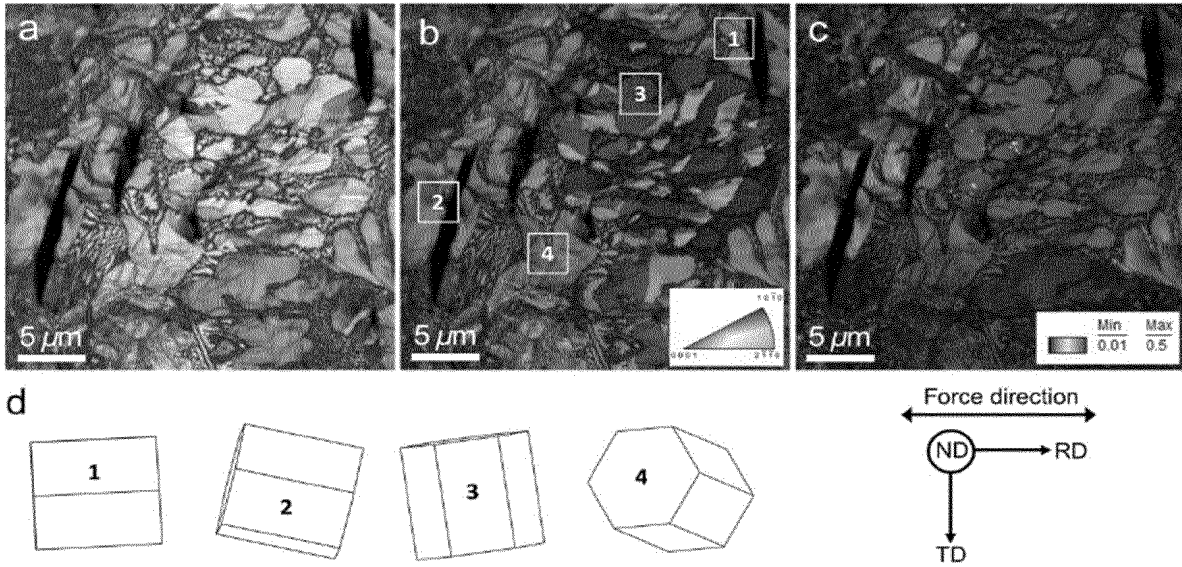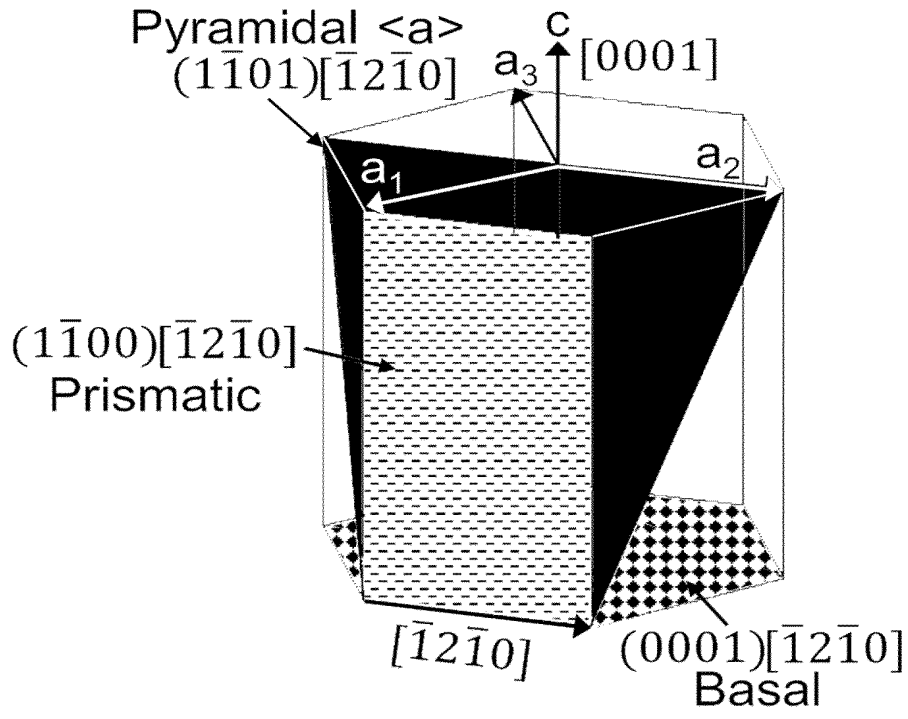
FIG 1.
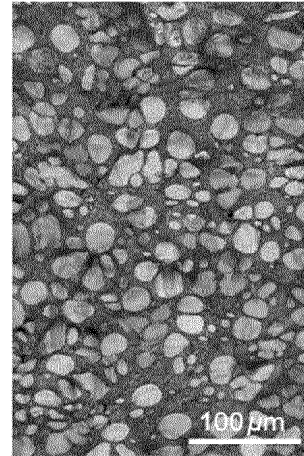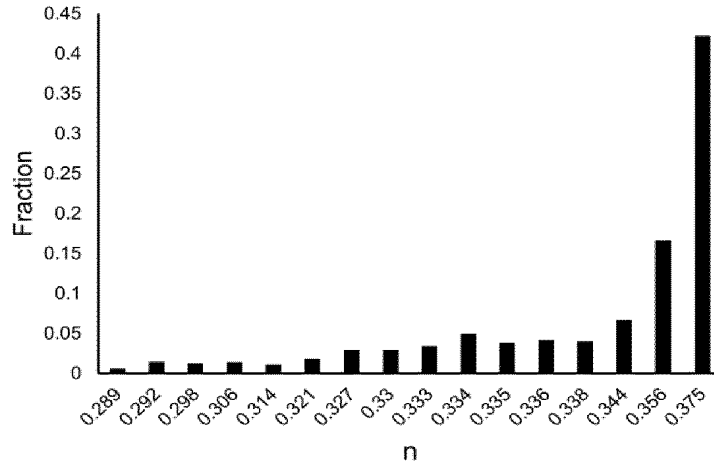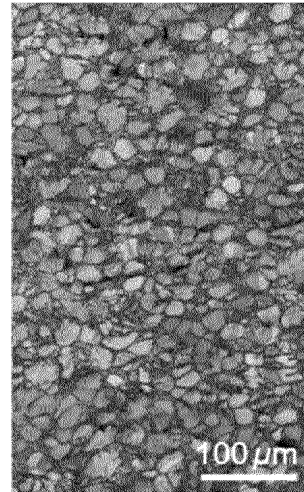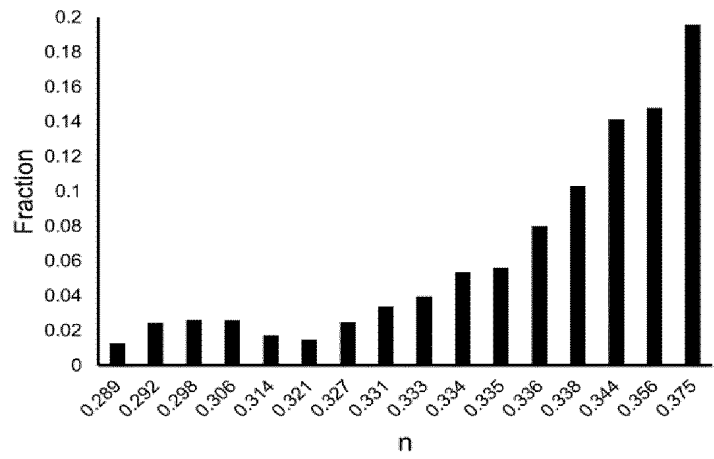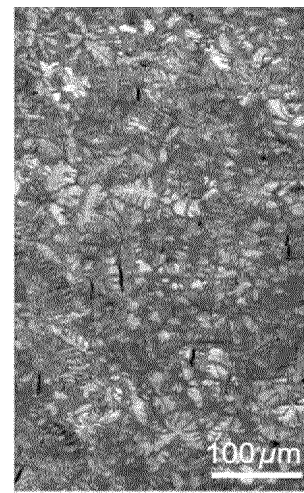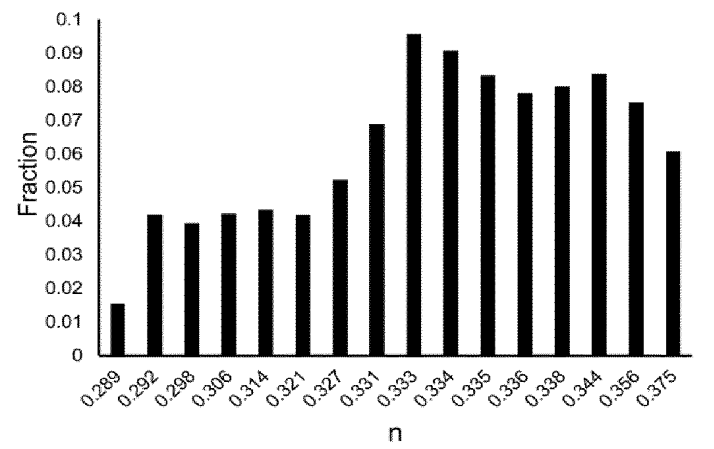
a

b

c

FIG 2.

FIG 3.

FIG 4.

FIG. 5

INTERNATIONAL SEARCH REPORT

A. CLASSIFICATION OF SUBJECT MATTER
INV. C22C18/00   C23C2/06   C23C22/40
ADD.

According to International Patent Classification (IPC) or to both national classification and IPC

B. FIELDS SEARCHED

Minimum documentation searched (classification system followed by classification symbols)

C22C C23C

Documentation searched other than minimum documentation to the extent that such documents are included in the fields searched

Electronic data base consulted during the international search (name of data base and, where practicable, search terms used)

EPO-Internal, WPI Data

C. DOCUMENTS CONSIDERED TO BE RELEVANT

Category*	Citation of document, with indication, where appropriate, of the relevant passages	Relevant to claim No.
Y	EP 2 088 219 A1 (JFE GALVANIZING & COATING CO [JP]; JFE STEEL CORP [JP]) 12 August 2009 (2009-08-12) claims 1-7; figures 1-9; tables 1-4 -----	1-13
Y	WO 2019/125020 A1 (POSCO [KR]) 27 June 2019 (2019-06-27) claims 1-7; figures 1-3; examples 1-7; table 1 -----	1-13
A	WO 2013/022118 A1 (JFE GALVANIZING & COATING CO LTD [JP]; JFE STEEL CORP [JP] ET AL.) 14 February 2013 (2013-02-14) claims 1-4; figures 1-2; tables 1-2 -----	1-13

-/--

[X] Further documents are listed in the continuation of Box C.   [X] See patent family annex.

```
*  Special categories of cited documents :

"A" document defining the general state of the art which is not considered
    to be of particular relevance
"E" earlier application or patent but published on or after the international
    filing date
"L" document which may throw doubts on priority claim(s) or which is
    cited to establish the publication date of another citation or other
    special reason (as specified)
"O" document referring to an oral disclosure, use, exhibition or other
    means
"P" document published prior to the international filing date but later than
    the priority date claimed
```

```
"T" later document published after the international filing date or priority
    date and not in conflict with the application but cited to understand
    the principle or theory underlying the invention
"X" document of particular relevance; the claimed invention cannot be
    considered novel or cannot be considered to involve an inventive
    step when the document is taken alone
"Y" document of particular relevance; the claimed invention cannot be
    considered to involve an inventive step when the document is
    combined with one or more other such documents, such combination
    being obvious to a person skilled in the art
"&" document member of the same patent family
```

Date of the actual completion of the international search	Date of mailing of the international search report
1 October 2020	14/10/2020

Name and mailing address of the ISA/ European Patent Office, P.B. 5818 Patentlaan 2 NL - 2280 HV Rijswijk Tel. (+31-70) 340-2040, Fax: (+31-70) 340-3016	Authorized officer Liu, Yonghe

C(Continuation).   DOCUMENTS CONSIDERED TO BE RELEVANT

Category*	Citation of document, with indication, where appropriate, of the relevant passages	Relevant to claim No.
A	A GHOSH AND N P GURAO: "Evolution of deformation heterogeneity at multiple length scales in a strongly textured zinc layer on galvanized steel", IOP CONF. SER.: MATER. SCI. ENG., vol. 82, 2015, pages 1-5, XP002794787, DOI: 10.1088/1757-899X/82/1/012024 page 1 - page 5	1-13

1

INTERNATIONAL SEARCH REPORT
Information on patent family members

Patent document cited in search report		Publication date	Patent family member(s)		Publication date
EP 2088219	A1	12-08-2009	CN	101558182 A	14-10-2009
			CN	104561874 A	29-04-2015
			EP	2088219 A1	12-08-2009
			JP	5101249 B2	19-12-2012
			JP	5661698 B2	28-01-2015
			JP	2008138285 A	19-06-2008
			JP	2012251246 A	20-12-2012
			KR	20090063216 A	17-06-2009
			MY	154537 A	30-06-2015
			SG	189593 A1	31-05-2013
			TW	200837219 A	16-09-2008
			US	2010086806 A1	08-04-2010
			WO	2008056821 A1	15-05-2008
WO 2019125020	A1	27-06-2019	CN	111511954 A	07-08-2020
			EP	3730663 A1	28-10-2020
			KR	20190077199 A	03-07-2019
			WO	2019125020 A1	27-06-2019
WO 2013022118	A1	14-02-2013	AU	2012293118 A1	20-02-2014
			CN	103732780 A	16-04-2014
			JP	5649181 B2	07-01-2015
			JP	2013036094 A	21-02-2013
			KR	20140043471 A	09-04-2014
			MY	165649 A	18-04-2018
			SG	2014007579 A	28-03-2014
			TW	201307612 A	16-02-2013
			WO	2013022118 A1	14-02-2013